A Simple Model to Explain ^{19}F-TDPAD Amplitude Characteristics *

H.-R. Blank, M. Frank, J. Heindl, M. Kaltenhäuser, H. Köchner, W. Kreische, N. Müller, S. Porscher, and T. Wagner

Physikalisches Institut der Universität Erlangen-Nürnberg, Erlangen, Germany

Z. Naturforsch. **47a**, 389–394 (1992); received July, 29, 1991

Since many years the ^{19}F-TDPAD method (TDPAD = time differential perturbed angular distribution) has been used to investigate electric field gradients in fluorine compounds. In these experiments always a strong reduction of the observed interaction amplitudes is observed. To explain these characteristics, a simple kinematic model is suggested.

Key words: TDPAD, Quadrupole interaction, Fluorine, Perturbation amplitude, Temperature dependence.

Introduction

This paper deals with the interpretation of ^{19}F-TDPAD amplitude data. For this purpose a short description of the TDPAD method will be given. Hereafter experimental results are reviewed and a simple kinematic model is suggested to explain the observed data. The features of the model will be discussed and possible improvements are mentioned in the last sections of the paper.

The following description of the TDPAD method is a short summary for the special case of ^{19}F probe nuclei. More general information is given in the literature [1–3].

In the special case of ^{19}F probe nuclei the angular distribution of the γ-radiation emitted by the transition from the second excited nuclear level ($E_x = 197$ keV, $I^\pi = 5/2^+$, $Q = 75$ mbarn, $\tau = 128.8$ ns) to the ground state is observed in a time differential manner. If all the m-sublevels of the excited state were equally populated, the radiation emission would be isotropic. However, the population of the excited level via the ^{19}F$(p,p')^{19}$F* nuclear reaction results in an alignment of the sublevels in beam direction.

The angular distribution of the emitted radition can be expanded into Legendre-Polynomials:

$$W(\theta) = \sum_{i=0}^{\infty} A_i \times B_i \times P_i(\cos\theta). \tag{1}$$

The distribution coefficients A_i depend on the transition matrix elements between the final and the initial nuclear state. The B_i are spin dependent factors describing the nuclear alignment. Due to general invariance principles the index i must be even and in the interval $0 \div 2I$. For $I = 5/2$ and using the abbreviation $A_{ii} := A_i \cdot B_i$ the angular distribution reduces to

$$W(\theta) = 1 + A_{22} \times P_2(\cos\theta) + A_{44} \times P_4(\cos\theta). \tag{2}$$

In an earlier paper [4] it was shown that for proton energies of ≈ 5 MeV the relation $A_{22} \approx 30 \cdot A_{44}$ holds. Within experimental errors as a good approximation the $i = 4$ terms may thus be neglected.

So far only the unperturbed angular distribution in a non-cubic environment has been described. The quadrupole moment of the excited level interacts with a EFG at the probe nucleus. This results in a time dependent perturbation $G_{22}(t)$ of the angular distribution:

$$W(\theta, t) = 1 + A_{22} \times G_{22}(t) \times P_2(\cos\theta),$$

$$G_{22}(t) = \sum_{n=0}^{3} s_{2n} \times \cos(\omega_n \times t). \tag{3}$$

The angular frequencies ω_n are given be the energy eigenvalues of the Hamiltonian describing the quadrupole interaction ($\omega_0 = 0$).

In the experiment the angular distribution is observed as a counting rate given by the product of $W(\theta, t)$ and the exponential decay of the excited level:

$$N'(\theta, t) = W(\theta, t) \times \exp(-t/\tau) + B = N(\theta, t) + B \tag{4}$$

* Presented at the XIth International Symposium on Nuclear Quadrupole Resonance Spectroscopy, London, United Kingdom, July 15–19, 1991.

Reprint requests to Prof. Dr. W. Kreische, Physikalisches Institut, Universität Erlangen-Nürnberg, Erwin-Rommel-Str. 1a, W-8520 Erlangen.

0932-0784 / 92 / 0100-0389 $ 01.30/0. – Please order a reprint rather than making your own copy.

B is a statistical background of random coincidences. Generally a ratio

$$R(t) = 2 \times \frac{N(180°, t) - c \times N(90°, t)}{N(180°, t) + 2 \times c \times N(90°, t)} = A_{22} \times G_{22}(t) \quad (5)$$

of the experimental data is formed to extract the perturbation. The factor c allows a correction for possible differences in the counter efficiences at 90° and 180°.

Results

In numerous experiments a great variety of fluorinated samples has been investigated. Generally only the quadrupole coupling constant ν_Q and the asymmetry parameter η were discussed. Besides this information, data about the effective interaction amplitudes A_{22}^{eff} are available from the experiments. Analyzing these, a characteristic dependence of the observed amplitude on the structure of the sample can be found.

In ionic crystals a relatively high amplitude (10% – 15%) was measured. This amplitude remains constant over the observed temperature range (up to 1100 K resp. T_m) within the experimental errors. Figure 1 illustrates this point with CuF_2 spectra taken at various temperatures showing nearly constant amplitudes. On the other hand, in molecular crystals relatively low amplitudes (2% – 6%) have often been found. These amplitudes decrease with increasing temperature. Figure 2 gives spectra for $CClF_3$, a typical molecular crystal. In Fig. 3 the data for a number of substances are summarized. The observed amplitudes are plotted versus the electronegativity difference between fluorine and the corresponding partner, a measure of the ionic character of the fluorine bond. The behaviour of the amplitudes in molecular crystals is contradicting the general experience gained in metals, where the corresponding amplitudes increase with increasing temperature [5]. At low temperatures the defects created by the nuclear recoil lead to a spread in the field gradient values. With increasing temperature the defects heal out and the amplitude of the corresponding undisturbed EFG component increases. This behaviour is not observed in insulators. Therefore radiation damages cannot explain the experimental data. Since A_{22} is given by nuclear properties it must be independent of the special crystal structure and the sample temperature. Special effects like thermal spikes can be neglected here. The amplitude of the modulation of $R(t)$ is proportional to the number of probe nuclei exposed to a distinct EFG (for the sake of simplicity in argumentation the occurrence of only one EFG is assumed here). In order to take this into account, $A_{22} \cdot G_{22}(t)$ is multiplied by a factor f, representing that fraction. The factor f may well depend on the crystal structure and the temperature of the sample. So (5) will be rewritten as

$$R(t, T) = f(T) \times A_{22} \times G_{22}(t). \quad (6)$$

The following considerations aim at finding a simple model for an analytical expression of $f(T)$. To do so, the scenario during the slowing down of the nuclei is shortly described.

Most of the incident protons are stopped in the target without performing a nuclear reaction. Only a few hit a fluorine nucleus and excite it to the 197 keV level. The ^{19}F* then moves through the target with a recoil energy in the keV range. It will also be slowed down in the target, initially dissipating most of its kinetic energy by electronic interaction. At lower velocities, nuclear collisions become the dominant stopping process. Three main types of collision may occur [6]:

1) Distruction collisions: The ^{19}F* hits a molecule and disintegrates it. This process may lead to a bond between the fluorine and fractional parts of the destroyed molecule. Therefore in some cases EFGs not expected from the constitution of the original target may be observed. This type of collision is only possible in molecular crystals.

2) The ^{19}F* pushes another atom off its site, leaving a vacancy.

3) The ^{19}F* recoil particle pushes another ^{19}F off its site and gets captured in the vacancy (replacement collision).

Only processes of type 3 contribute to the fraction of probe nuclei that experience the unperturbed EFG. So, in order to determine $f(T)$ the probability of type 3 collisions has to be calculated.

To perform these calculations some simplifying assumptions are made:

1) Even though the transition from the region where electronic stopping is dominant to the one where nuclear stopping is the relevant process is continuous, a sharp transition at a threshold energy E_{max} is assumed.

2) The probability of a collision at energy $E_1 < E_{\text{max}}$ is taken constant.

3) For ionic crystals it is assumed that ions are bond to the crystal with energy E_b; transfering kinetic energy greater than E_b to an atom will push it off its site.

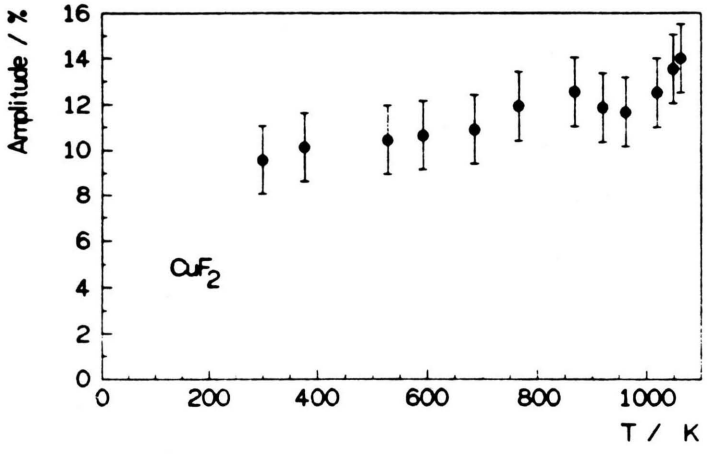

Fig. 1. Observed amplitude for the ionic crystal CuF_2 vs. T.

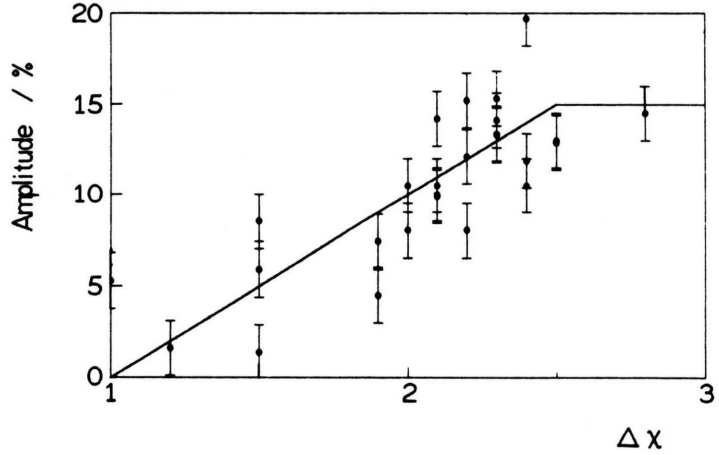

Fig. 3. Maximum amplitudes vs. electronegativity difference of the fluorine bond for a variety of substances. The solid lines are eye-guides.

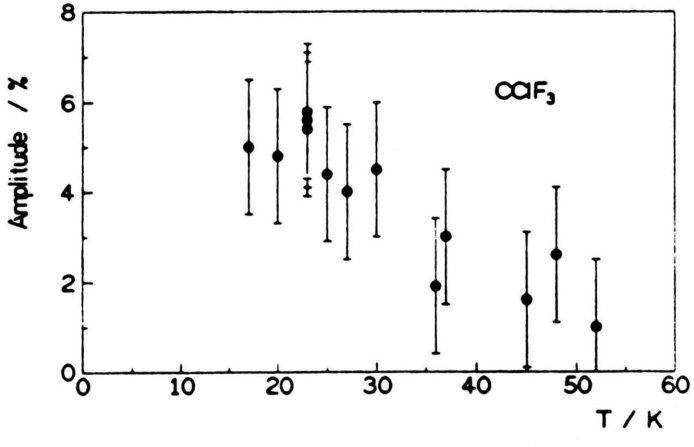

Fig. 2. Observed amplitude for the molecular crystal $CClF_3$ vs. T.

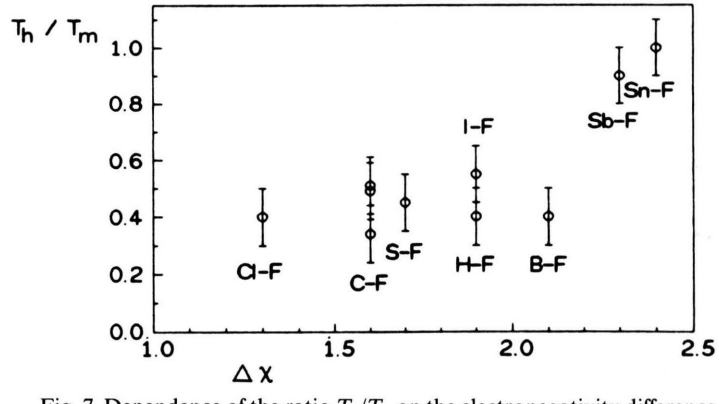

Fig. 7. Dependence of the ratio T_h/T_m on the electronegativity difference of the indicated bonds.

4) In molecular crystals two relevant binding energies must be considered. On the one hand the atoms are bound to their molecules via a bond energy E_b, on the other hand the molecules themselves are bound in the crystals as a whole by the van-der-Waals energy E_c.

Using these simplifications, f can be calculated from kinematic considerations.

A) Ionic Crystals

Regarding a collision between the incident ^{19}F* and a target ^{19}F, the conservation of energy and linear momentum has to be satisfied:

$$\begin{aligned} \boldsymbol{p}_{-1} &= \boldsymbol{p}'_{-1} + \boldsymbol{p}'_{-2}, \\ E_1 &= E'_1 + E'_2. \end{aligned} \tag{7}$$

Indices 1 and 2 denote the projectile and the target particle; the primes denote the corresponding quantities after the collision.

Solving these equations for E'_1 and E'_2 yields

$$\begin{aligned} E'_1 &= E_1 \times \cos^2 \Phi, \\ E'_2 &= E_1 \times \sin^2 \Phi, \end{aligned} \tag{8}$$

where $\cos \Phi = \boldsymbol{p}_{-1} \cdot \boldsymbol{p}'_{-1} / p_1 \cdot p'_1$.

A replacement collision can take place if $E'_2 > E_b$ and simultaneously $E'_1 < E_b$ is satisfied.

This leads to the condition

$$\frac{1}{\sin^2 \Phi} \leqq \frac{E_1}{E_b} \leqq \frac{1}{\cos^2 \Phi}. \tag{9}$$

In Fig. 4 this condition is fulfilled in the dotted region. The ratio of the dotted area to the whole area surrounded by the dashed line gives the fraction of projectiles that can perform replacement collision (averaging with respect to $\sin \Phi$ has been taken into account):

$$f_1 = \frac{(2 \times x_1)^{1/2} - 2.295}{x_1}, \tag{10}$$

where $x_1 = E_{max}/E_b$.

Since E_b is in the order of some eV and E_{max} in the range of 10 to 100 eV, no considerable variation of f with the temperature T occurs, thermal energies being in the order of some 10^{-2} eV.

B) Molecular Crystals

In molecular crystals the collision kinematics are the same as in ionic crystals but an additional condition occurs. If a replacement collision has taken place, the remaining energy E'_1 of the caught projectile is assumed to be distributed over the whole molecule. If this energy is greater than or comparable to the van der Waals energy E_c with which the molecule is bound in the crystals, the local environment of the probe nucleus will be highly distorted so that no distinct EFG may be observable. The additional condition $E'_1 < E_c$ for the observability of a EFG after a replacement collision can be formulated as

$$\frac{E_1}{E_b} \leqq \frac{E_c}{E_b} \times \frac{1}{\cos^2 \Phi}. \tag{11}$$

The fraction of incident projectiles satisfying (9) and (11) is shown as the dotted area in Figure 5. For the fraction f of projectiles that contribute to the dotted area again integration and averaging with respect to Φ has to be performed. It has to be kept in mind that collisions occur only below the upper limit E_{max}. This

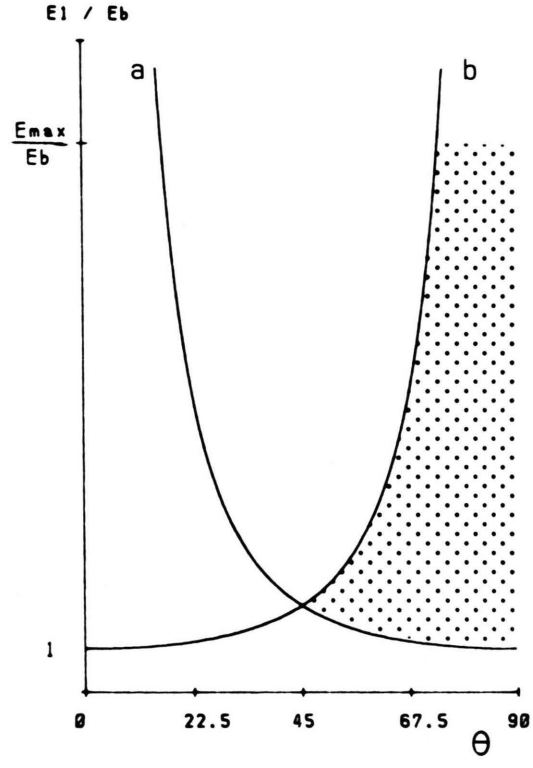

Fig. 4. Dependence of E'_1 and E'_2 of the collision angle θ (schematic plot). Only the marked region contributes to the observable amplitude.

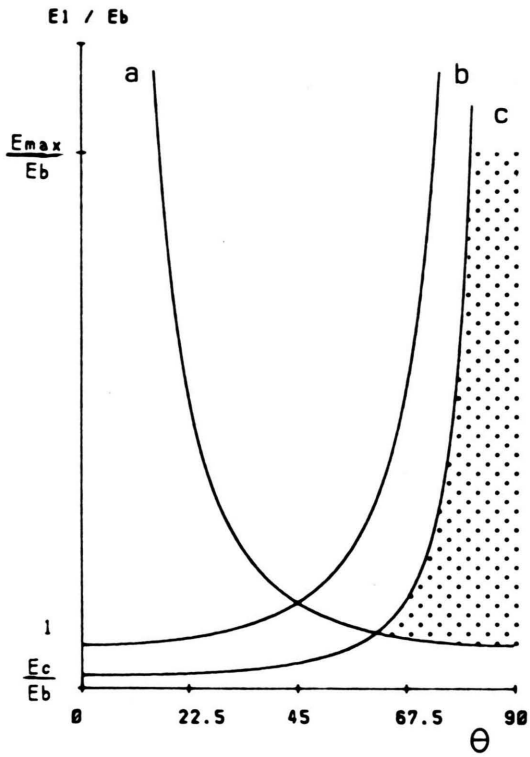

Fig. 5. The same quantities as in Fig. 4 are shown, but additionally the condition of (11) is drawn. Again the region that contributes to the amplitude is shaded.

yields:

$$f_M = \left[\left(x_2 \times \left(\frac{x_1}{x_2}\right)^{1/2} - \left(1+\frac{1}{x_2}\right)^{1/2}\right) + x_1 \times \left(\frac{x_2}{x_1}\right)^{1/2} + \ln\left((1+x_2)^{1/2} - x_2^{1/2}\right)\right] \Big/ x_1, \tag{12}$$

where $x_2 = E_c/E_b$; $x_1 = E_{max}/E_b$.

Here again the temperature dependence of x_1 is negligible. On the other hand the van der Waals energy E_c is in the order of typically 10 meV to 100 meV and therefore the influence of the temperature T on $E_c(T)$ has to be taken into account:

The simplest ansatz for the temperature dependence of E_c is given as

$$E_c(T) = E_{c0} \times \left(1 - \frac{T}{T_m}\right), \tag{13}$$

where T_m is the melting temperature of the substance.

In Fig. 6 $V = f_I(0)/f_M(0)$ is shown for some parameter sets x_2 as a function of $x_1 = E_{max}/E_b$.

The obtained formulae for f_I and f_M can describe the important features of the experimentally obtained TDPAD amplitudes:

1. In ionic crystals no temperature dependence occurs.

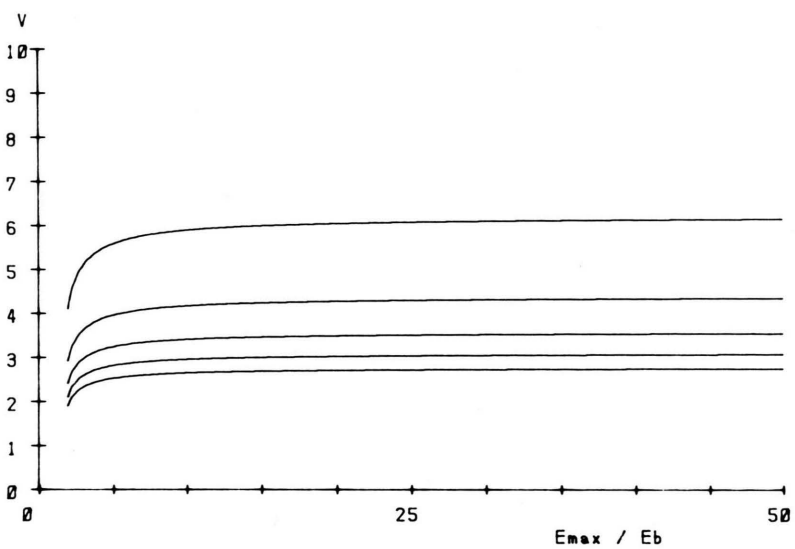

Fig. 6. Plot of $V = f_I(0)$ vs. $x_1 = E_{max}/E_b$. The parameter E_{c0}/E_b takes the values 0.025, 0.05, 0.75, 0.1, 0.125 (from top to bottom line). For $x_1 > 5$ the ratio V is nearly independent of x_1. The values of V in this parameter range in agreement with the experimentally observed ones. V is practically independent of x_1, thus the exact choice of E_{max} is not crucial.

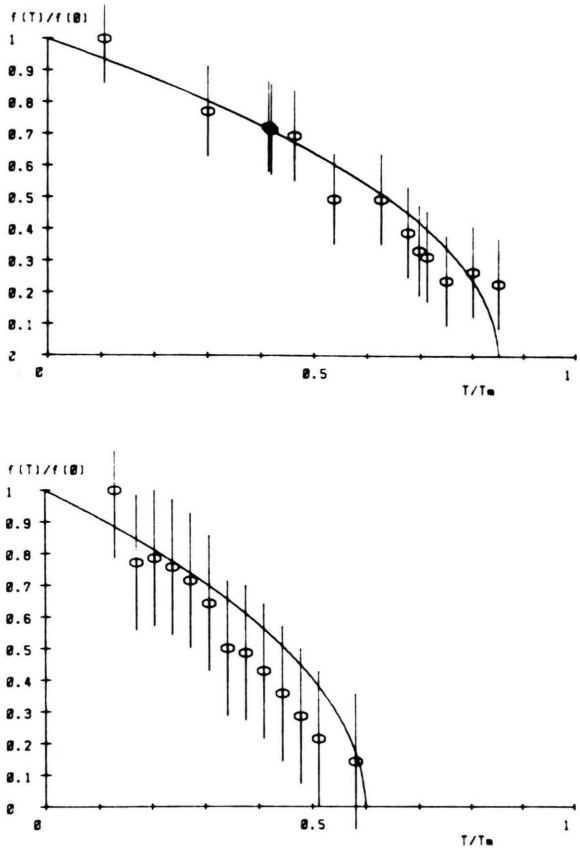

Fig. 8. Comparison between the model and experimentally observed data for IF_5 (top) and BF_3 (bottom) in a normalized plot.

2. In molecular crystal $f_M(T)$ and therefore the observable amplitude decreases with increasing temperature.

3. In the low temperature limit the ratio f_M/f_I yields values between two and six, depending on the actual parameters.

4. A characteristic measure of the decay of the amplitudes in molecular crystals with increasing temperature, the temperature T_H, where the amplitude reaches half its maximum value, is defined. In Fig. 7 T_H/T_m is shown for a number of substances. As can be seen, this ratio has a value of ≈ 0.4, independent of the special sample. According to our model one expects a constant value for T_H/T_m, only determined by the ansatz (13) for the temperature dependence of $E_c(T)$ and therefore constant for all substances.

Conclusion

The model suggested above is capable of describing the experimentally observed features of the ^{19}F-TDPAD amplitudes qualitatively, some even quantitatively. Due to the fact that in the model only one collision in the energy range $0 \leqq E_1 \leqq E_{max}$ is considered, it seems not too strange that the absolute f-values are smaller than the observed ones. On the other hand, from Monte-Carlo simulations [7] it is known that in the mentioned range approximately 4–5 collisions occur. This number corresponds very closely to the factor between the f-factors of the model and the relative experimental amplitudes.

The obtained formula for f_M is based on the assumption that if E_1' after a replacement collision is comparable to E_c, no distinct EFG is observable due to the highly distorted local environment of the probe nuclei in these cases. However, this causes f_M to disappear at T_m. To get rid of this rather artificial restriction it might be better to introduce an energy $E_s \leqq E_c$ at which the above situation should occur. This may be taken into account by a modified ansatz for x_2:

$$x_2(T) = \begin{cases} E_{c0} \times \left(1 - \dfrac{T}{T_s}\right) & \text{for} \quad T \leqq T_s \\ 0 & \text{else,} \end{cases} \tag{14}$$

where T_m is replaced by T_s.

Figure 8 shows a comparison between experimental data and model curves vor IF_5 and BF_3.

Finally it can be stated that the model describes the experimentally observed data in a satisfactory manner. It is based on some intuitive assumptions and simple kinematics. Future work will have to be done to improve details of the model.

[1] H. Frauenfelder and R. M. Steffen, Alpha-, Beta- and Gamma-Ray Spectroscopy, Vol. 2, North-Holland, Amsterdam 1965.
[2] R. M. Steffen and K. Alder, The Electromagnetic Interaction in Nuclear Spectroscopy, North-Holland, Amsterdam 1975.
[3] H. Morinaga, and T. Yamazaki, In-Beam Gamma-Ray Spectroscopy, North-Holland, Amsterdam 1976.
[4] W. Kreische, H. Niedrig, K. Reuter, K. Roth, and K. Thomas, Phys. Rev. C **17**, 2006 (1978).
[5] H. Haas, Physica Scripta **11**, 221 (1975).
[6] M. Frank, F. Gubitz, W. Kreische, A. Labahn, Ch. Ott, B. Röseler, F. Schwab, and G. Weeske, Hyp. Int. **34**, 259 (1987).
[7] J. Ziegler, Trim 90, Software-package.